LAWRENCE
LIVERMORE
NATIONAL
LABORATORY

LLNL-PROC-415001

SHOCKLESS LOADING WITH RECOVERY FOR CHARACTERIZATION OF MATERIAL RESPONSE

J. M. McNaney, B. Torralva, K. T. Lorenz, B. A. Remington, M. Wall, M. Kumar

July 23, 2009

Shock compression of condensed matter 2009
Nashville, TN, United States
June 28, 2009 through July 3, 2009

Disclaimer

SHOCKLESS LOADING WITH RECOVERY FOR CHARACTERIZATION OF MATERIAL RESPONSE

J. M. MCNANEY, B. TORRALVA, K. T. LORENZ, B. A. REMINGTON, M. WALL, M. KUMAR

Lawrence Livermore National Laboratory, L-356, Livermore CA 94551

Abstract. A new recovery based method for investigating material response to non-Hugoniot loading paths is described. The work makes use of a laser generated plasma piston that produces ramped loading at high strain rates ($>\approx 10^7$/s). Large sample sizes are utilized to prevent reflected wave interactions. The overall deformation path is characterized by two transients: one at very high strain rate on the 5-10 nanosecond time scale and one at a lower strain rate occurring over a 1-2 microsecond timescale. It was found that a sufficiently large region of material experiences shockless loading conditions such that recovery based characterization is feasible. The presence of two strain transients makes the method more applicable to comparative assessments between shockless and shock loading conditions.

Keywords: shockless, recovery, high strain rate
PACS:

INTRODUCTION

Many studies over the past 4-5 decades (e.g. see [1-2]) have considered the response of materials to shock loading. These studies have generally used gas gun or high explosive (HE) driven impactors to load the material to pressures up to a few tens of GPa and have deployed material recovery and subsequent characterization to assess deformation response. The strain, temperature and strain rate are almost exclusively determined by the peak shock pressure as dictated by the equation of state. While very high shock pressures are routinely attainable on both lasers (up to 75 TPa) and the Z-machine (Sandia National Laboratory, up to 500 GPa), melting generally limits *solid state* materials studies [3-8] on these platforms to ≈100-200 GPa. The laser driven experiments have utilized high-intensity, direct illumination of the material, over nanosecond timescales, to create a shock driven by material ablation while the Z-machine uses a temporally shaped magnetic pulse to either compress materials directly or accelerate a projectile impactor. More recently, shockless drives based on lasers [3,9], HE [10,11] and gas guns [12] have been developed which allow control over both the drive pressure and loading rate.

The current work describes a laser-based method to investigate the effect of a ramped loading path on the observed deformation response of the solid material at very high strain rates. The ability to investigate material response in this regime can yield insight into both the deformation mechanisms and the transition from thermal activation controlled response to other phenomena (e.g., drag limited mobility, homogeneous dislocation nucleation).

EXPERIMENTAL

The laser based drive, schematically presented in Figure 1, begins with a high power laser pulse creating an ablation-driven shock wave in a reservoir of material (typically a polymer or carbon foam). The passage of the strong shock sets the reservoir into motion. As the shock exits the rear of the reservoir, the material releases as a weakly ionized plasma and moves toward the sample,

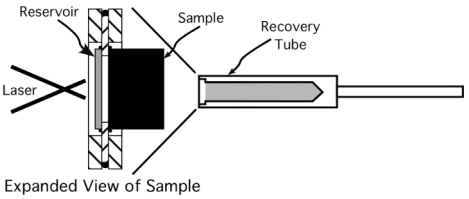

Figure 1. Schematic of reservoir and sample arrangement showing an expanded view of the drive geometry.

which is situated some distance away across a vacuum gap. At the same time, the head of the unloading (rarefaction) wave travels back into the compressed reservoir material at the local sound speed. The unloading process stretches out the plasma so that a gently rising pressure pulse is generated as the plasma piles up against the sample. The resultant compressive loading follows a quasi-isentropic (shockless) path, which eventually steepens into a shock wave as it propagates through the sample. Additional details concerning the drive are described in [9].

All experiments were carried out on the Omega Laser located at the Laboratory for Laser Energetics (University of Rochester, NY). As shown schematically in figure 1, the sample was placed in a drive "package" facing and separated from a reservoir by a shim washer to create the necessary evacuated gap as described above. This drive package was placed in a tube to facilitate recovery of the sample.

Generation of the drive was achieved by focusing three beams on an approximately 500 μm diameter region of the ablator side of a laminate reservoir. The reservoir consisted of a 150 μm thick region of polystyrene (with 2.5 atomic % Br) and a 25 μm region of opaque polyimide (Kapton® CB) ablator material joined with a thin layer of adhesive resulting in a total thickness of ≈180 μm. A reservoir material containing bromine was used to prevent pre-heating of the copper sample by x-rays generated at the ablation front. The beams were conditioned, in order to smooth the spatial intensity profile, through the use of phase plates resulting in an on target spot profile wherein the intensity remained within 90% of its peak value over ≈ 500 μm (800 μm FWHM) [13].

A square laser pulse, 3.5 – 3.7 ns in duration, having a beam intensity of 10.5 x 10^{12} w/cm^2 or 13.3 x 10^{12} w/cm^2 on the reservoir surface, was used to generate a peak pressure pulse, at the sample surface, of approximately 25 GPa or 40 GPa respectively. Drive calibration was provided through a series of experiments described in [9] where peak pressures between 15 and 100 GPa were considered. Subsequent to this experimental corroboration, hydrodynamics modeling was used to simulate the global, time-dependent test history, as described below.

The material studied was single crystal copper (99.999% purity), in the form of a right circular cylinder, 3 mm in diameter and 3 mm thick. The crystal was oriented such that the normal to the (001) plane was parallel to the drive axis. It should be noted that the size and thickness of the samples investigated herein resulted in dissipation of the loading wave such that the region of interest, near the sample surface and facing the drive, was essentially unaffected by reflected shock waves.

While the mechanistic response of the material will be considered in a future publication, the current work makes use of global deformation as a benchmarking tool for development of the overall methodology.

RESULTS AND DISCUSSION

The entire experiment was modeled with the hydrodynamics simulation code CALE [14]. A two-dimensional axi-symmetric model was used to simulate the experiment. A simple constitutive model [15] was employed in modeling the continuum deformation response. These continuum calculations provide detailed information on the generation of the plasma "piston" used to load the sample, as well as the associated momentum transfer and wave propagation through the sample. Salient features of the loading based on the results of the simulations, including the shockless/shock transition as well as plasma-surface interactions, are described below. An overview of the simulation is presented in Figure 2.

The simulated global deformation response well matches the experimentally observed crater depth for the sample loaded to 25 GPa, as can be seen in figure 3. The overall deformation process occurs over the timescale of about 1 μs with the bulk of the crater formation process occurring in the first 0.8 μs.

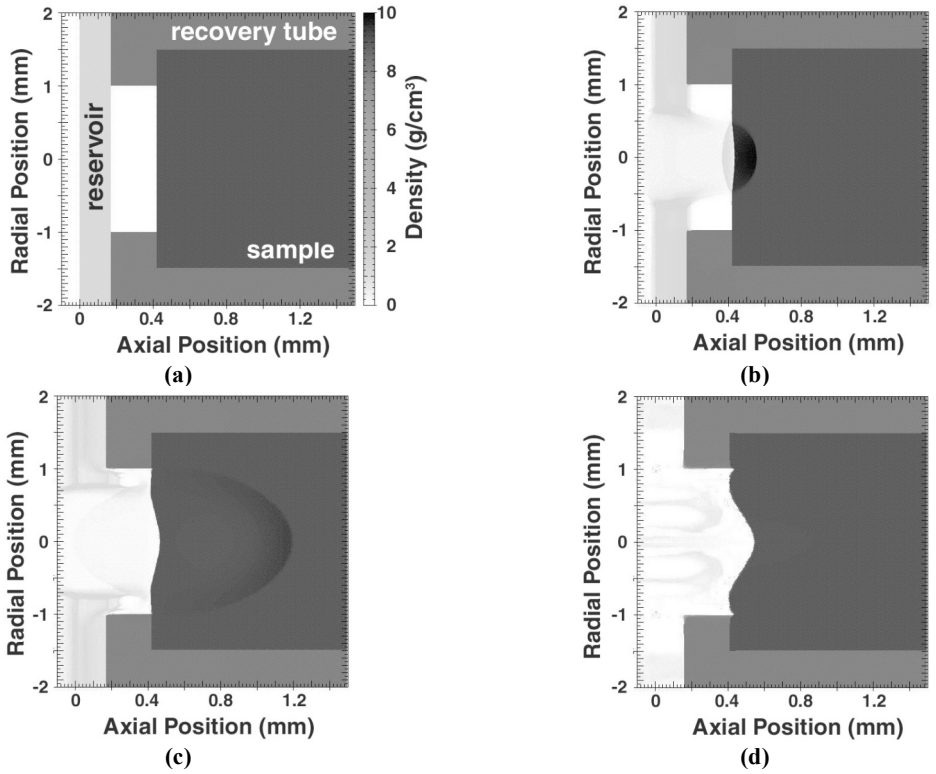

Figure 2. Density plots showing progression of the simulation at (a) t=0, (b) 60ns, (c) 200ns, (d) 2 μs for the 25 GPa peak loading case.

The stress on the front face of the sample is constrained to follow the incident pressure pulse, which is induced by the reservoir plasma, as described above. As the pressure wave travels through the material it steepens and eventually becomes a shock. This transition to shock loading, shown in figure 4, is accompanied by an increase in temperature relative to the shockless region. The transition occurs over the region 80-110 μm below the crater surface in the case of the 25 GPa sample and 30-60 μm below the crater surface in the case of the 40 GPa. The increase in temperature, as the path moves from shockless to shock loading, is evident. Although it is more difficult to ascertain the transition by inspection of the pressure loading curve (figure 4b), careful observation reveals that the front of the wave attains a steady state, much steeper profile in the shock region.

As can be seen (Fig. 4), the temperature rises during the pressure transient due mostly to compressional heating and falls as the pressure wave passes. While temperatures in the shocked region during the 40 GPa transient approach 550 °K, due to the increase in melt temperature with pressure, the homologous temperature, T/T_{melt}, remains below 0.2 with residual temperatures ≈ 0.31. In comparison, the shockless region experiences a peak temperature of ≈ 0.13 with a residual temperature of ≈ 0.24. The 40 GPa case provides an upper bound for comparison between the shockless and shock loading since the temperature excursions and residual temperatures in the case of the 25 GPa loading are lower. When comparing the behavior of the material in the shockless and shock loaded regions, the temperature effects on the deformation response would be expected to be small.

One drawback of the current methodology is that the small drive spot makes it difficult to employ momentum trapping techniques that are required to achieve one-dimensional loading throughout the recovery process. This is demonstrated by the presence of a crater in the

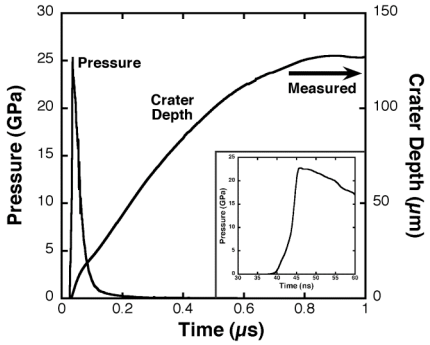

(a)

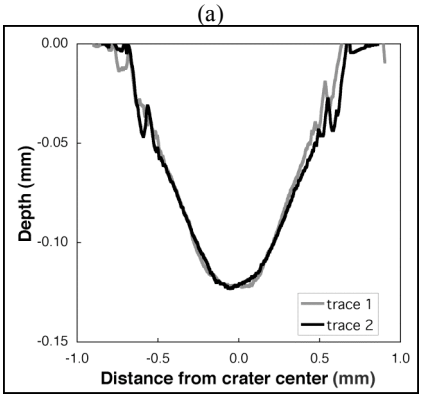

(b)

Figure 3. (a) Pressure and crater depth as a function of time from the simulation. Measured final crater depth from a sample loaded to 25 GPa and recovered is shown with horizontal arrow. Inset shows initial loading occurs over a ≈ 10 ns period. (b) Profilometry traces through the center of the crater in a sample recovered from 25 GPa loading at the Omega laser.

sample. As can be seen in figure 5a, much of the strain is accumulated after the passage of the high pressure loading transient. A concomitant effect of this deformation chronology is the wide range of strain rates experienced by the sample. As seen in figure 5b, where the strain rates for the ramp driven region have been plotted as a function of time. The strain rate can vary by almost an order of magnitude throughout the process, even larger for the shock driven regions. Still, it should be kept in mind that both shockless and shocked regions experience essentially the same strain and pressure history so that comparisons between the two regions yield a valuable comparative assessment of the effect of loading paths off the shock Hugoniot.

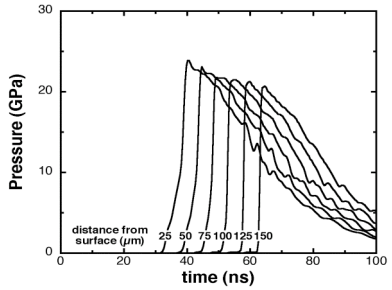

(a)

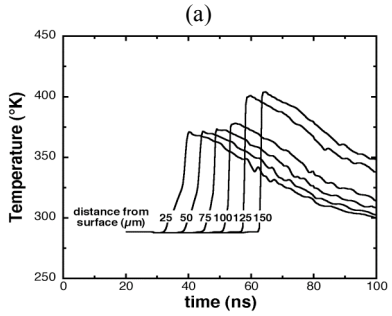

(b)

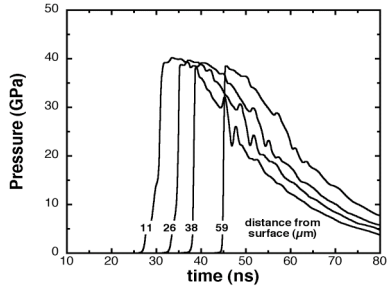

(c)

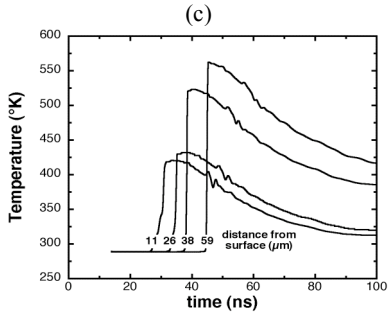

(d)

Figure 4. Simulation results showing (a) Pressure and (b) temperature profiles as a function of time at depths of 25, 50, 75, 100, 125, and 150 μm for the 25 GPa sample. (c) Pressure and (d) temperature profiles as a function of time at 11, 26, 38, and 59 for the 40 GPa sample. While the transition from shockless to shock loading is not easily defined from pressure profiles it is evident in the temperature change.

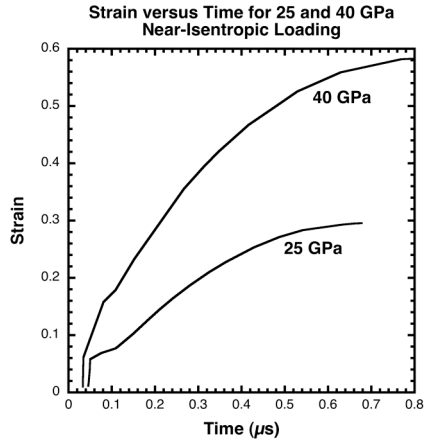

(a)

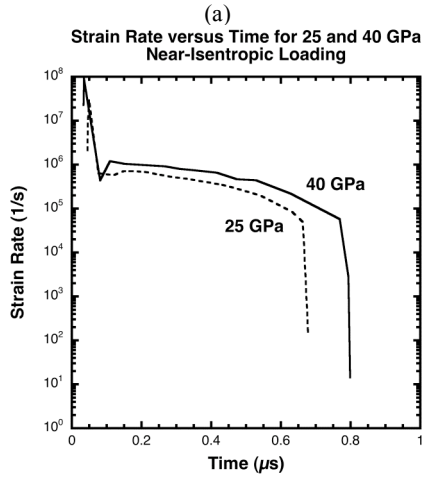

(b)

Figure 5. Plots of (a) strain and (b) strain rate for the quasi-isentropically loaded material as a function of time based on simulation results. Note that the strain rates peak during the passage of the wave and that significant strain is accumulated at lower strain rates after the passage of the high pressure wave.

CONCLUSIONS

A new laser based recovery based method for investigating material response to non-Hugoniot loading paths has been described. Large sample sizes are utilized to prevent reflected wave interactions. The overall deformation path is characterized by two transients: one at very high strain rate on the 5-10 nanosecond time scale and one at a lower strain rate occurring over a 1-2 microsecond timescale. The similarity of pressure and strain paths of material experiencing shockless and shocked loading allows for post-recovery characterization of the effect of loading path on material response.

ACKNOWLEDGEMENTS

This work was performed under the auspices of the U.S. Department of Energy by Lawrence Livermore National Laboratory, in part under Contract W-7405-Eng-48, and in part under Contract DE-AC52-07NA27344.

REFERENCES

1. Gray III G. T. in: Shock-wave and high strain-rate phenomena, 1992 (Meyers MA, Murr LE, Staudhammer KP, eds.), pp. 899-911.
2. Murr L. E., Esquivel E. V., J. Mater. Sci. 39, 1153, 2004.
3. Lorenz K. T., et. al., Phys. of Plas. 12, 056309/1-11, 2005.
4. Kalantar D. H., et. al., Wiley L. G. American Institute of Physics Conference Proceedings, no.505, pt.2, 2000, pp. 1193-7.
5. Meyers M. A., et. al., Acta Mat. 51, 1211, 2003.
6. Hall C. A., Phys. Plas., 7, 2069, 2000.
7. Hall C. A., et. al., Rev. Sci. Instrum., 72, 3587, 2001.
8. Reisman D. B., et. al., J App Phys., 89, 1625, 2001.
9. Edwards M. J., et. al., Phys. Rev. Let., 92, 075002/1, 2004.
10. Barnes J. F., et. al., J. App. Phys., 45, 727, 1974.
11. Lebedev A. I., Nizovtsev P. N., Raevskii V. A., Solov'ev, V. P., Dokl. Akad. Nauk 349 (MAIK Nauka/Interperiodica Publishing, Moscow (1996)). Translation:Phys. Dokl., 41, 328, 1996.
12. Nguyen J. H., Orlikowski D., Streitz F. H., Holmes N. C., Moriarty J. A., in Shock Comp. Cond. Matt. 2004 (Furnish MD, Chhabildas LC, and Hixson RS, eds.). AIP Conf. Proc., no. 706 pt. 2, pp. 1225-30.
13. Glendinning et. al., Phys. Plasmas, 10, 1931, 2003.
14. Tipton R., Managan R., Amala P., 2002. CALE Users Manual. Lawrence Livermore National Laboratory.
15. Steinberg D. J., Cochran S. G., Guinan M. W., J. Appl. Phys., 51, 1498, 1980.